

Observer-Based Backstepping Controller Design for Gear Shift Control of a Seamless Clutchless Two-Speed Transmission for Electric Vehicles*

Mir Saman Rahimi Mousavi, *Member, IEEE*, Ali Pakniyat, *Member, IEEE*
Mohamed K. Helwa, *Member, IEEE*, Benoit Boulet, *Senior Member, IEEE*

Abstract—This paper proposes an observer-based backstepping controller design for gear shifting control of a seamless and clutchless two-speed transmission for electric vehicles. The state observer estimates the input and output torques of the transmission and the angular velocities of the gears, based on measuring the motor speed and the speed of the vehicle. Then, an observer-based backstepping controller is designed to provide seamless gear change while tracking the optimal trajectory corresponding to the minimum shifting time. Thereafter, the separation of the estimation and control is discussed. The driveline of an electric vehicle is modeled in MATLAB/Simulink by utilizing SimDriveLine library components to asses the performance of the designed observer and controller.

Index Terms—backstepping controller; minimum order observer; seamless two-speed transmission; electric vehicles

I. INTRODUCTION

Fuel cost and environmental concerns have pushed the automotive industry to gradually replace internal combustion engine (ICE) vehicles with hybrid electric vehicles (HEV) and fully electric vehicles (EV). However, the energy density of electric batteries is much less than that of fossil fuels. Hence, by changing the source of power, it is required to minimize the losses in the driveline in order to maximize the range of EVs. Using multi-speed transmission for EVs can reduce the size of the electric motor and improve dynamic performance and efficiency of the driveline [1]. In particular, gear changing decision can be employed by the controller to optimize the vehicle's performance measures [2–6].

Currently used transmissions for EVs were mostly designed for vehicles with ICEs. As is well known, ICEs cannot operate below certain speeds and their speed control during gear changes is rather complicated and therefore, the presence of clutches or torque convertors is inevitable for the vehicle lurching and gear changing. This, however, is not the case for EVs as electric motors are speed controllable in a wide range of operating speeds. This difference, in fact, provides an opportunity for designing novel transmissions as the one proposed in [2], [7]. This transmission has the advantage of maintaining the output speed and torques during the gear shift and is able to eliminate the problem of lacking traction during gear change and the issues raising from sudden re-engagements of the synchronizer; problems which are inevitable in clutchless AMTs [8], [9] that reduce

passenger comfort and the lifetime of the transmission [10–16]. The elimination of output torque interruptions during gear changing is similar to the special features of DCTs [17], while the considered design benefits a higher efficiency and a lower weight compared to them.

In an earlier work (see [7]), a seamless and clutchless two-speed transmission particularly designed for EVs is presented in order to provide an appropriate balance between efficiency and dynamic performance of the vehicle. Moreover, a similar control method as for DCTs and ATs via torque and inertia phases is applied to provide smooth gearshifts [18–21]. In [2] a more detailed dynamic modeling of the proposed transmission is presented and the Pontryagin Minimum Principle is used in order to optimize the shifting time. Figure 1 shows the schematic view of the driveline of an electric vehicle equipped with the proposed in [2], [7]. The transmission system, as it is shown in Fig. 1, is comprised of a dual-stage planetary gear set with common ring and common sun gears. Two friction brakes are used to control the flow power.

In this paper, the kinematic analysis of the dual-stage planetary gear set, the achievable gear ratios of the transmission, and the dynamical model of the driveline of an electric vehicle equipped with the proposed transmission in [2], [7] are reviewed. The flexibility of the half shafts and longitudinal vehicle dynamics are taken into the consideration in the presented dynamical model of the system. In order to reduce the number of sensors for measuring the required speeds and torques for the closed-loop control laws introduced in [2], [7], a minimum order observer is designed to estimate the unmeasured states. The observer estimates the speeds of the on-coming and off-going gears and the input and output torques of the transmission based on the measured speeds of the motor and the vehicle. Due to nonlinearities in the system such as the longitudinal vehicle dynamics, nonlinear observer methods generally apply for the observer design. However, as shown in this paper, a minimum order observer can be designed in such a way that the nonlinear dynamics of the vehicle are eliminated form the error dynamics of the estimation by injecting the nonlinear term in the dynamic equation of the observer. Furthermore, an observer-based nonlinear backstepping controller is designed in order to provide seamless gear shifting while tracking the optimal trajectory which minimizes the shifting time. The driveline of an electric vehicle is modeled in MATLAB/Simulink® by utilizing SimDriveLine library for the performance validation of the designed observer and the backstepping controller for gear shift control.

*This work was supported by Automotive Partnership Canada (APC).

M.S Rahimi Mousavi, A. Pakniyat, M. K. Helwa, and B. Boulet are with the Centre for Intelligent Machines (CIM) and the Department of Electrical Engineering, McGill University, Montréal, QC H3A 2T5, Canada, saman@cim.mcgill.ca.

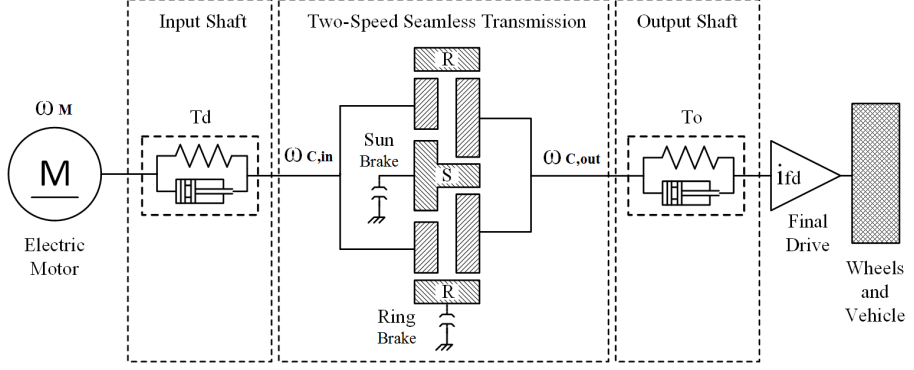


Fig. 1. Schematic view of an electric vehicle driveline equipped with the proposed seamless clutchless two-speed transmission

II. PRELIMINARIES

A. Kinematic Equations

The kinematic relations between planetary gear components such as Carrier (C), Sun (S), Planets (P), and Ring (R) for this transmission are derived in [2], [7] as follows:

$$\begin{cases} \omega_{C,in} = \frac{R_1\omega_R + \omega_S}{(R_1 + 1)}; & \omega_{C,out} = \frac{R_2\omega_R + \omega_S}{(R_2 + 1)} \\ \omega_{P,in} = \frac{R_1\omega_R - \omega_S}{(R_1 - 1)}; & \omega_{P,out} = \frac{R_2\omega_R - \omega_S}{(R_2 - 1)} \end{cases} \quad (1)$$

where the variables ω_S , ω_P , ω_R , and ω_C are the angular velocities of the sun, planets, ring, and carrier, respectively, while R_1 and R_2 are

$$R_1 := \left(\frac{r_R}{r_S}\right)_{input}; \quad R_2 := \left(\frac{r_R}{r_S}\right)_{output} \quad (2)$$

where r_S and r_R are the pitch radii of the sun and ring gears, respectively.

B. Achievable Gear Ratios

According to equations set (1), the speed ratio of the output of the transmission to the input can be expressed as follows:

$$\frac{\omega_{C,out}}{\omega_{C,in}} = \frac{(R_1 + 1)(\omega_S + R_2\omega_R)}{(R_2 + 1)(\omega_S + R_1\omega_R)} \quad (3)$$

According to (3), three different gear ratios are achievable:

- 1) If the ring is completely grounded ($\omega_R = 0$):

$$\frac{\omega_{C,out}}{\omega_{C,in}} = \frac{(R_1 + 1)}{(R_2 + 1)} = GR_1 \quad (4)$$

- 2) If the sun is completely grounded ($\omega_S = 0$):

$$\frac{\omega_{C,out}}{\omega_{C,in}} = \frac{(R_1 + 1)R_2}{(R_2 + 1)R_1} = GR_2 \quad (5)$$

- 3) If neither the sun nor the ring is completely grounded ($\omega_R \neq 0$ and $\omega_S \neq 0$):

$$\frac{\omega_{C,out}}{\omega_{C,in}} = \frac{(R_1 + 1)(\omega_S + R_2\omega_R)}{(R_2 + 1)(\omega_S + R_1\omega_R)} = GR_T \quad (6)$$

Here, GR_1 and GR_2 are the first and the second gear ratios, while GR_T is the transient gear ratio between the first and the second gears. The term upshift and downshift refer to going from the first gear ratio to the second and from the second to the first, respectively.

C. Dynamic Modeling of the Driveline

A more detailed dynamical model of the driveline of an electric vehicle equipped with the transmission in [2], [7], [22] can be represented as follows by considering flexibility of the half shafts, longitudinal vehicle dynamics, and viscous friction in the transmission:

$$\begin{aligned} \dot{\omega}_w &= \frac{-T_v}{J_v} + \frac{i_{fd}}{J_v} T_o \\ \dot{\omega}_M &= \frac{-1}{J_M} T_d + \frac{1}{J_M} T_M \\ \dot{\omega}_S &= \frac{-C_S \tau}{a} \omega_S + \frac{C_R \lambda}{a} \omega_R + \frac{c}{a} T_d - \frac{d}{a} T_o \\ &\quad + \frac{\tau}{a} (T_{BS} + T_{SF}) - \frac{\lambda}{a} (T_{BR} + T_{RF}) \\ \dot{\omega}_R &= \frac{C_S \lambda}{a} \omega_S - \frac{C_R \gamma}{a} \omega_R + \frac{e}{a} T_d - \frac{f}{a} T_o \\ &\quad - \frac{\lambda}{a} (T_{BS} + T_{SF}) + \frac{\gamma}{a} (T_{BR} + T_{RF}) \\ \dot{T}_d &= K_d \omega_M - \frac{K_d}{R_1 + 1} \omega_S - \frac{K_d R_1}{R_1 + 1} \omega_R \\ \dot{T}_o &= -i_{fd} K_o \omega_w + \frac{K_o}{R_2 + 1} \omega_S + \frac{K_o R_2}{R_2 + 1} \omega_R \end{aligned} \quad (7)$$

where T_M , T_d , T_o , and T_v are the electromagnetic torque of the motor, the torque of the input shaft, the output torque of the transmission, and the road load torque. Angular velocities of the motor and wheels are denoted by ω_M and ω_w , respectively. In equation (7), the constants C_S , C_R , T_{SF} and T_{RF} are the coefficients of the Coulomb and viscous friction of the transmission and can be measured from experimental tests. The final drive ratio of the driveline is denoted by i_{fd} . The terms T_{BS} and T_{BR} are the torque brakes of the sun and ring gears, respectively. The coefficients α , β , γ , τ , λ , ϕ , ψ , a , c , d , and f in the equation (7) are listed in Table I. The inertia of the motor, sun, ring, input carrier, output carrier, input planets, output planets, and the vehicle and wheels are J_M , I_S , I_R , $I_{C,in}$, $I_{C,out}$, $I_{P,in}$, $I_{P,out}$, and J_v , respectively. The mass of the input and output planets are denoted by $m_{P,in}$ and $m_{P,out}$. Slip of the tires are neglected so the geometric relation $v_x = R_w \omega_w$ can be considered between the speed of the tires for the straight motion.

The input torque (T_d) and output torque (T_o) of the

TABLE I
THE COEFFICIENT OF THE DYNAMICAL MODELING (7)

$\alpha = \frac{(I_{C,in} + 4m_{P,in}r_{C,in}^2)}{(R_1+1)^2}$	$\phi = \frac{4I_{P,in}}{(R_1-1)^2}$
$\beta = \frac{(I_{C,out} + 4m_{P,out}r_{C,out}^2)}{(R_2+1)^2}$	$\psi = \frac{4I_{P,out}}{(R_2-1)^2}$
$\gamma = [I_S + \alpha + \beta + \phi + \psi]$	$a = (\gamma\tau - \lambda^2)$
$\tau = [I_R + (\alpha + \phi)R_1^2 + (\beta + \psi)R_2^2]$	$c = \frac{\tau - R_1\lambda}{R_1+1}$
$\lambda = [(\alpha - \phi)R_1 + (\beta - \psi)R_2]$	$d = \frac{\tau - R_2\lambda}{R_2+1}$
$e = \frac{\gamma R_1 - \lambda}{R_1+1}$	$f = \frac{\gamma R_2 - \lambda}{R_2+1}$

transmission can be calculated as follows:

$$\begin{aligned} T_d &= K_d(\theta_M - \theta_{C,in}) + B_d(\omega_M - \omega_{C,in}) \\ T_o &= K_o(\theta_{C,out} - i_{fd}\theta_w) + B_o(\omega_{C,out} - i_{fd}\omega_w) \end{aligned} \quad (8)$$

where K_d and K_o are the equivalent torsional stiffness and B_d and B_o are the damping constants of the input and output shafts. The road load torque (T_v) can be calculated from the following relation [17]:

$$T_v = R_w \left(\frac{1}{2} \rho v_x^2 C_d A_f + m_v g \sin(\theta_r) + K_r m_v g \cos(\theta_r) \right) \quad (9)$$

where R_w , θ_r , K_r , m_v , v_x , ρ , C_d , g , and A_f indicate wheel radius, road angle, tire rolling resistance, vehicle mass, vehicle velocity, air density, aerodynamic drag coefficient, gravitational acceleration, and vehicle frontal area.

The brake of the sun is designed to be of the multi-plate brake type. Thus, the relation between the normal applied force on the friction plates and the resulting torque is [23]:

$$T_{BS} = -\mu_P N_{BS} n \left(\frac{2}{3} \right) \left(\frac{R_o^3 - R_i^3}{R_o^2 - R_i^2} \right) \text{sign}(\omega_S); \quad N_{BS} \geq 0 \quad (10)$$

where μ_P is the coefficient of friction between brake plates, N_{BS} is the normal force applied to the plates, n is the number of the friction surfaces, and $\text{sign}(\cdot)$ is the signum function. The inner and outer radii of the multi-plate brakes are expressed as R_i and R_o , respectively. The brake of the ring is designed to be of band brake type. So, the relation between the normal applied force at the end of the band and the resulting torque is [23]:

$$\begin{cases} T_{BR} = -N_{BR} R_D (e^{\mu_D \theta} - 1); \omega_R \geq 0, & N_{BR} \geq 0 \\ T_{BR} = N_{BR} R_D (1 - e^{-\mu_D \theta}); \omega_R < 0, & N_{BR} \geq 0 \end{cases} \quad (11)$$

where N_{BR} is the force applied at the end of the band, R_D is the radius of the drum brake, μ_D is the coefficient of friction between band and drum and θ is the angle of wrap.

III. OBSERVER DESIGN

From (7) and (9), the system is apparently nonlinear because of the nonlinear dynamics for the ω_w , and so nonlinear observer design is required to construct the system states for full-state feedback control methods. Since the vehicle speed and the motor speed are continuously measured, the values of

ω_w and ω_M are known at all instants. Hence, minimum order observers can be defined in such a way that the nonlinear term is eliminated from the error dynamics by injecting the known nonlinear term in the dynamics of the observer.

In order to design a minimum order observer, the states of the system (7) are broken down into two sets of available ($x_a(t)$) and unavailable ($x_u(t)$) states as follows:

$$\begin{aligned} \begin{bmatrix} \dot{x}_a(t) \\ \dot{x}_u(t) \end{bmatrix} &= \begin{bmatrix} A_{aa} & A_{au} \\ A_{ua} & A_{uu} \end{bmatrix} \begin{bmatrix} x_a(t) \\ x_u(t) \end{bmatrix} + \begin{bmatrix} B_a \\ B_u \end{bmatrix} u(t) + \begin{bmatrix} E_a \\ E_u \end{bmatrix} T_v \\ y(t) &= [\mathbf{I}_{[2 \times 2]} \quad \mathbf{0}_{[2 \times 4]}] \begin{bmatrix} x_a(t) \\ x_u(t) \end{bmatrix} \end{aligned} \quad (12)$$

where the states $x_a(t)$, $x_u(t)$, and the inputs $u(t)$ are

$$x_a(t) = \begin{bmatrix} \omega_w \\ \omega_M \end{bmatrix}, \quad x_u(t) = \begin{bmatrix} \omega_S \\ \omega_R \\ T_d \\ T_o \end{bmatrix}, \quad u(t) = \begin{bmatrix} T_M \\ T_{BS} + T_{Sf} \\ T_{BR} + T_{Rf} \end{bmatrix}, \quad (13)$$

and matrices A_{aa} , A_{au} , A_{ua} , A_{uu} , B_a , B_u , E_a , and E_u are:

$$\begin{aligned} A_{aa} &= \begin{bmatrix} 0 & 0 \\ 0 & 0 \end{bmatrix}, \quad A_{au} = \begin{bmatrix} 0 & 0 & 0 & \frac{i_{fd}}{J_v} \\ 0 & 0 & \frac{-1}{J_M} & 0 \end{bmatrix}, \\ A_{uu} &= \begin{bmatrix} \frac{-C_S \tau}{a} & \frac{C_R \lambda}{a} & \frac{c}{a} & \frac{-d}{a} \\ \frac{C_S \lambda}{a} & \frac{-C_R \gamma}{a} & \frac{e}{a} & \frac{-f}{a} \\ \frac{-K_d}{R_1+1} & \frac{-K_d R_1}{R_1+1} & 0 & 0 \\ \frac{K_o}{R_2+1} & \frac{K_o R_2}{R_2+1} & 0 & 0 \end{bmatrix}, \\ A_{ua} &= \begin{bmatrix} 0 & 0 \\ 0 & 0 \\ 0 & K_d \\ -i_{fd} K_o & 0 \end{bmatrix}, \quad B_u = \begin{bmatrix} 0 & \frac{\tau}{a} & \frac{-\lambda}{a} \\ 0 & \frac{-\lambda}{a} & \frac{\gamma}{a} \\ 0 & 0 & 0 \\ 0 & 0 & 0 \end{bmatrix}, \\ B_a &= \begin{bmatrix} 0 & 0 & 0 \\ \frac{1}{J_M} & 0 & 0 \end{bmatrix}, \quad E_a = \begin{bmatrix} -\frac{1}{J_v} \\ 0 \end{bmatrix}, \quad E_u = [\mathbf{0}]_{[4 \times 1]}. \end{aligned} \quad (14)$$

The minimum order observer equation is as follows [24]:

$$\begin{aligned} \dot{\tilde{x}}_u(t) &= (A_{uu} - LA_{au}) \tilde{x}_u(t) + (A_{ua} - LA_{aa}) x_a(t) \\ &\quad + L \dot{x}_a(t) + (E_u - LE_a) T_v + (B_u - LB_a) u(t) \end{aligned} \quad (15)$$

where L is the observer gain. Let $e_u = x_u - \tilde{x}_u$ denote the error in the estimated states. From (12) and (15), the error dynamics can be written as follows:

$$\dot{e}_u(t) = (A_{uu} - LA_{au}) e_u(t) \quad (16)$$

which is asymptotically stable if the matrix $A_{uu} - LA_{au}$ has all its eigenvalues in the open left half plane. A sufficient condition for the existence of such L is that (A_{au}, A_{uu}) is observable. It can be shown that the observability matrix for (A_{au}, A_{uu}) is full rank and such L exists. Estimating $x_u(t)$ from (15) requires differentiating $x_a(t)$ which is not desirable. To eliminate this problem, the following change of variables is considered:

$$\tilde{z}(t) = \tilde{x}_u(t) - L x_a(t) = \tilde{x}_u(t) - L y(t) \quad (17)$$

Hence, the estimation of $x(t)$ is:

$$\tilde{x}(t) = \begin{bmatrix} y(t) \\ \tilde{z}(t) + L y(t) \end{bmatrix}. \quad (18)$$

IV. BACKSTEPPING CONTROLLER TO TRACK THE OPTIMAL TRAJECTORY

The control inputs of the driveline are the electromagnetic torque of the motor T_M , the sun brake T_{BS} , and the ring brake T_{BR} . In [2] the Pontryagin Minimum Principle (PMP) was applied on this system in order to find the optimal control law which minimizes the shifting time of the transmission. The result of the PMP problem for this transmission results in a sudden engagement and a sudden disengagement of the on-coming and off-going brakes and an optimal trajectory for T_d . Here, T_{BS} and T_{BR} follow the same trend mentioned in [2] while coping with physical constraints such as actuator limitation. Moreover, a backstepping controller is designed in such a way that T_d exponentially converges to the optimal trajectory in [2]. Rearranging the second and the fifth equations in (7) gives:

$$\begin{cases} \dot{T}_d = -K_d\omega_{C,in} + K_d\omega_M \\ \dot{\omega}_M = -\frac{T_d}{J_M} + \frac{T_M}{J_M} \end{cases} \quad (19)$$

where the control input is T_M , and by observing ω_S and ω_R , $\omega_{C,in}$ is available from (1). Considering the scalar equation

$$\dot{T}_d = -K_d\omega_{C,in} + K_d\omega_M \quad (20)$$

and designing a feedback control law which makes

$$\omega_M = \varphi(T_d) = \omega_{C,in} + \frac{\dot{T}_{d_{des}} - K_I(T_d - T_{d_{des}})}{K_d}, \quad (21)$$

result in

$$\dot{T}_d = \dot{T}_{d_{des}} - K_I(T_d - T_{d_{des}}). \quad (22)$$

Considering the following candidate Lyapunov function:

$$V_1(T_d) = \frac{1}{2}(T_d - T_{d_{des}})^2, \quad (23)$$

and applying the virtual control (21) make the Lyapunov function derivative negative definite:

$$\dot{V}_1(T_d) = -K_I(T_d - T_{d_{des}})^2 \leq 0, \text{ for } K_I > 0 \quad (24)$$

which ensures that $T_d \rightarrow T_{d_{des}}$ as $t \rightarrow \infty$.

Now, using the backstepping change of variables:

$$\zeta = \omega_M - \varphi(T_d) \Leftrightarrow \omega_M = \varphi(T_d) + \zeta, \quad (25)$$

transfers the system (19) to:

$$\begin{cases} \dot{T}_d = -K_I(T_d - T_{d_{des}}) + \dot{T}_{d_{des}} + K_d\zeta \\ \dot{\zeta} = -\dot{\varphi}(T_d) + \frac{T_M - T_d}{J_M} \end{cases} \quad (26)$$

Considering the second Lyapunov function as follows

$$V_2(T_d, \zeta) = \frac{1}{2}(T_d - T_{d_{des}})^2 + \frac{1}{2}\zeta^2 \quad (27)$$

and choosing the electromagnetic torque of the motor as:

$$T_M = T_d + \dot{\varphi}(T_d)J_M - K_d(T_d - T_{d_{des}})J_M - K_{II}J_M \\ \left(\omega_M - \omega_{C,in} - \frac{\dot{T}_{d_{des}} - K_I(T_d - T_{d_{des}})}{K_d} \right), \quad K_{II} > 0 \quad (28)$$

ensure the stability of the system (26) by making the derivative of the Lyapunov function (27) negative definite

$$\dot{V}_2(T_d, \zeta) = -K_I(T_d - T_{d_{des}})^2 - K_{II}\zeta^2 \quad (29)$$

which clearly ensures that $(T_d, \zeta) \rightarrow (T_{d_{des}}, 0)$ as $t \rightarrow \infty$. So, the trajectories of the system asymptotically converge to the optimal one in [2].

V. SEPARATION OF THE ESTIMATION AND CONTROL

As discussed in Section III, ω_w and ω_M are the only measured states. Thus, to implement (28) in practice, the actual values of the rest of the states should be replaced with their estimated values. Since the considered system (7) is nonlinear, the straightforward separation principle for linear systems does not apply here. Instead, the following argument is presented which shows that the overall system (with the observer) achieves the desired control objective. To that end, the augmented state is defined as $x_{aug} := [x \ e_u]^T \in \mathbb{R}^{10}$, where $x = [\omega_w \ \omega_M \ \omega_S \ \omega_R \ T_d \ T_o]^T \in \mathbb{R}^6$, and $e_u \in \mathbb{R}^4$ is the error in the estimated state as discussed before. The dynamics of the augmented system are given by (7) and (16). First, some observations are made on the augmented system. Notice that during the upshift (or the downshift), T_{BS} and T_{BR} are continuous functions in time, and that the augmented dynamics can be expressed as $\dot{x}_{aug} = f(t, x_{aug})$, where f is continuous in time and locally Lipschitz in x_{aug} (uniformly in time). From Theorem 3.1 of [25], for each initial condition $x_{aug_0} \in \mathbb{R}^{10}$ and under the proposed control law, there exists a unique solution of the augmented system, denote it $\phi(t, x_{aug_0})$. Also, from Theorem 3.5 of [25], $(t, x_{aug_0}) \mapsto \phi(t, x_{aug_0})$ is a continuous function. It can be verified that in the case of this paper, the augmented system does not have a finite escape time, so the trajectory $\phi(t, x_{aug_0})$ is defined for all $t \in [0, \infty)$. Second, consider the subspace $S := \{x_{aug} \in \mathbb{R}^{10} : e_u = 0\}$. It is shown that for each $x_{aug_0} \in S$, $\phi(t, x_{aug_0})$ remains in S for all $t \in [0, \infty)$, and the control objective is achieved, i.e. $(T_d, \xi) \rightarrow (T_{d_{des}}, 0)$ as $t \rightarrow \infty$. From (16), if $e_u = 0$, then $\dot{e}_u = 0$, and so S is invariant. In particular, for each $x_{aug_0} \in S$, $\phi(t, x_{aug_0}) \in S$ for all $t \in [0, \infty)$. On S , $e_u(t) = 0$, i.e. the control law (28) is accurate, and (29) is valid. Thus, $(T_d, \xi) \rightarrow (T_{d_{des}}, 0)$ as $t \rightarrow \infty$. Third, let $x_{aug_0} \in \mathbb{R}^{10}$, $x_{aug_0} \notin S$ be arbitrary. It is shown that $\phi(t, x_{aug_0}) \rightarrow S$ as $t \rightarrow \infty$, and $(T_d, \xi) \rightarrow (T_{d_{des}}, 0)$ as $t \rightarrow \infty$. Since the transversal dynamics to S given by (16) are asymptotically stable, then $e_u(t) \rightarrow 0$ as $t \rightarrow \infty$. Equivalently, $\phi(t, x_{aug_0}) \rightarrow S$ as $t \rightarrow \infty$. It is claimed that $\phi(t, x_{aug_0})$ is bounded. Suppose by contradiction that $\|\phi(t, x_{aug_0})\| \rightarrow \infty$ as $t \rightarrow \infty$. By triangle inequality and since $e_u(t) \rightarrow 0$ as $t \rightarrow \infty$, it can be concluded that $\|x(t)\| \rightarrow \infty$ as $t \rightarrow \infty$. On the other hand, it is known that $\phi(t, x_{aug_0}) \rightarrow S$ as $t \rightarrow \infty$, and on S the system is asymptotically stable. This clearly contradicts continuity of the state trajectories of the augmented system with respect to initial conditions. Notice that as time evolves, T_{BS} and T_{BR} become constant values in finite time, and the

augmented dynamics become autonomous. Since $\phi(t, x_{aug_0})$ is bounded, then by Birkhoff's Theorem [26], the positive limit set for the initial condition x_{aug_0} , denoted $L^+(x_{aug_0})$, is nonempty, compact (closed and bounded), invariant (both positively invariant and negatively invariant), connected, and $\phi(t, x_{aug_0}) \rightarrow L^+(x_{aug_0})$ as $t \rightarrow \infty$. It is shown that $L^+(x_{aug_0}) \subset S$. Let $\bar{x}_{aug} \in L^+(x_{aug_0})$ be arbitrary. By definition of a limit set, it is known that there exists a sequence $\{t_i\}$ with $t_i \rightarrow \infty$ such that $\phi(t_i, x_{aug_0}) \rightarrow \bar{x}_{aug}$. In particular, $e_u(t_i) \rightarrow \bar{e}_u$, the vector consisting of the last four components of \bar{x}_{aug} , as $t_i \rightarrow \infty$. But, it is known that $e_u(t_i) \rightarrow 0$ as $t_i \rightarrow \infty$. Therefore, $\bar{e}_u = 0$ [27], and $\bar{x}_{aug} \in S$. Since $\bar{x}_{aug} \in L^+(x_{aug_0})$ is arbitrary, $L^+(x_{aug_0}) \subset S$. On S , the inequality (29) is valid, and so any compact, invariant set in S must lie in $\{x \in S : V_2(T_d, \xi) = 0\}$. Thus, $L^+(x_{aug_0}) \subset \{x \in S : V_2(T_d, \xi) = 0\}$, and so $(T_d, \xi) \rightarrow (T_{d_{des}}, 0)$ as $t \rightarrow \infty$.

VI. SIMULATION RESULTS

For the proposed transmission with parameters given in Table II, simulation results are provided for the upshift and downshift by using the MATLAB library SimDriveLine. The upshift and downshift start at $t = 7.4(s)$ and $t = 13.4(s)$ respectively, which according to Fig. 2 and Fig. 4, the shifting periods last around $0.5(s)$. Figure 2 shows the motor speed, the measured and estimated speeds of the ring and sun gears, the actual and the desired speed of the wheels before, during and after the upshift. The actual and estimated input and output torques of the transmission during the upshift are presented in Fig. 3. The motor speed, the measured and estimated speeds of the ring and sun gears, the actual and the desired speed of the wheels before, during and after the downshift operation are shown in Fig. 4. Figure 5 shows the actual and estimated torque of the input and output of the transmission during the downshift process. Negative torque in this figure shows that the electric motor goes on regeneration mode during the sample downshift. The small deviations of the estimated speeds of on-coming and off-going gears from the actual speeds come from the neglected terms of damping in the dynamical model (7) and the difference between the friction models for the brakes which are considered here and the friction models for the brakes in SimDriveLine in MATLAB. Simulation results show the observer effectively estimates unmeasurable states and the observer-based backstepping controller provides seamless gear shift such that the oscillations of the output torque and the deviation of the output speed from the desired speed remain less than 5% during the abrupt gear change process.

VII. CONCLUSION

In this paper, a minimum order state observer is designed in order to estimate the speed of on-coming and off-going gears and the input and output torque of the seamless two-speed transmission proposed for electric vehicles. Based on the measured and estimated states, a backstepping method is applied to design a controller to track the minimum shifting time trajectory presented in [2] while providing seamless

TABLE II
PARAMETERS OF THE DYNAMICAL SYSTEM

$r_{R,in}(m)$	6e-2	$I_R(Kg.m^2)$	9e-3
$r_{R,out}(m)$	6e-2	$I_S(Kg.m^2)$	1.5e-3
$r_{S,in}(m)$	3e-2	$I_{C,in}(Kg.m^2)$	1.4e-3
$r_{S,out}(m)$	15e-3	$I_{C,out}(Kg.m^2)$	0.1
$r_{P,in}(m)$	15e-3	$I_{P,in}(Kg.m^2)$	6.08e-6
$r_{P,out}(m)$	22.5e-3	$I_{P,out}(Kg.m^2)$	3.12e-5
$C_R(N.m.s/rad)$	0.001	$m_{P,in}(Kg)$	0.0512
$C_S(N.m.s/rad)$	0.001	$m_{P,out}(Kg)$	0.12113
$T_{Rf}(Nm)$	0.05	$T_{Sf}(Nm)$	0.05
μ_R, μ_S	0.15	n	4
$R_o(m)$	0.09	$R_i(m)$	0.08
$R_D(m)$	0.1	$\theta(rad)$	$3\pi/4$
$K_o(N/rad)$	10000	$J_V(Kg.m^2)$	70
$K_d(N/rad)$	10000	$A_f(m^2)$	3
$R_w(m)$	0.3	K_r	0.015
ρ	.005	i_{fd}	5

gear change. The simulation results verify the satisfactory performance of the designed minimum order observer and backstepping controller during the abrupt gear shift process.

It is worth mentioning that although the separation principle for linear systems does not apply in the case of this paper, however a rigorous argument is provided to indicate the separation of the estimation and control.

ACKNOWLEDGMENT

We gratefully acknowledge the support of our industrial partners: Linamar, TM4 and Infolytica. The research work

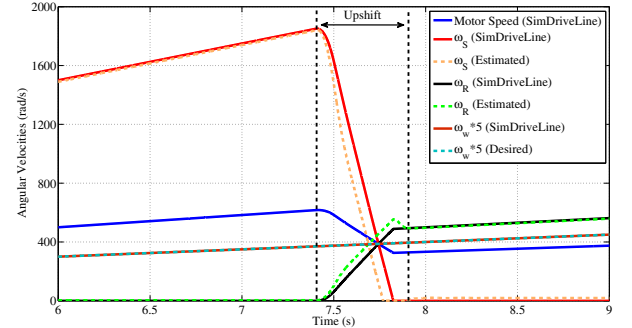


Fig. 2. Estimated and actual angular velocities (upshift operation)

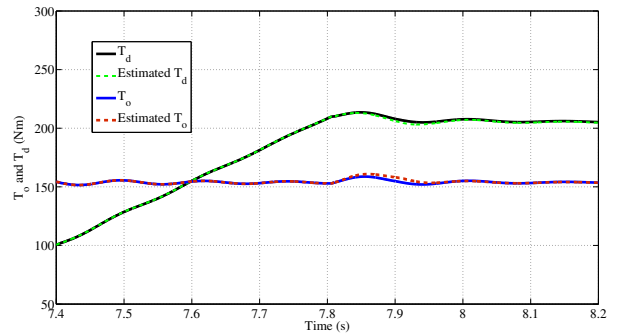


Fig. 3. Estimated and actual input and output torques (upshift operation)

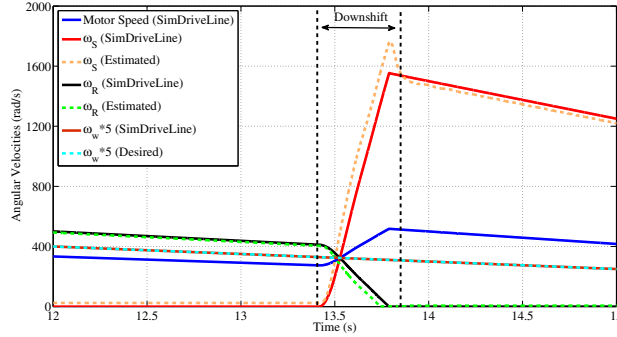


Fig. 4. Estimated and actual angular velocities (downshift operation)

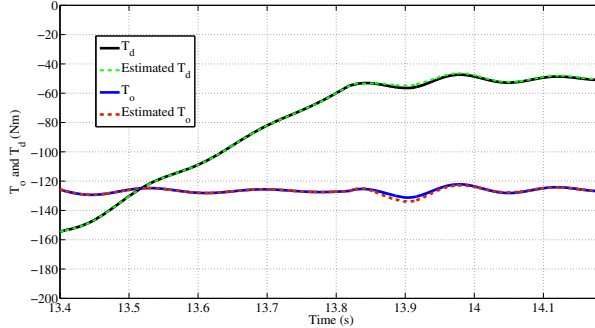


Fig. 5. Estimated and actual input and output torques (downshift operation)

reported here is supported by the Natural Sciences and Engineering Research Council of Canada (NSERC) and the Automotive Partnership Canada (APC).

REFERENCES

- [1] P. D. Walker, S. A. Rahman, B. Zhu, and N. Zhang, "Modelling, Simulations, and Optimisation of Electric Vehicles for Analysis of Transmission Ratio Selection", *Hindawi Publishing Corporation, Advances in Mechanical Engineering*, Vol. 2013.
- [2] M. S. Rahimi Mousavi, A. Pakniyat, B. Boulet, "Dynamic Modeling and Controller Design for a Seamless Two-Speed Transmission for Electric Vehicles", *IEEE Multi-Conference on Systems and Control*, Nice, France, 8-10 October 2014, pp. 635-640.
- [3] A. Pakniyat, P. E. Caines, "The Gear Selection Problem for Electric Vehicles: an Optimal Control Formulation", *13th International Conference on Control, Automation, Robotics and Vision, ICARCV 2014*, Marina Bay Sands, Singapore, December 2014, pp. 1261-1266.
- [4] A. Pakniyat, P. E. Caines, "Time Optimal Hybrid Minimum Principle and the Gear Changing Problem for Electric Vehicles", *5th IFAC Conference on Analysis and Design of Hybrid Systems, ADHS 2015*, Atlanta, GA, USA, October 2015.
- [5] Futang Zhu, Li Chen, Chengliang Yin, "Design and Analysis of a Novel Multimode Transmission for a HEV Using a Single Electric Machine", *IEEE trans. on vehicular technology*, vol. 62, no. 3, March 2013, pp. 1097-1110.
- [6] Yuan Cheng, R. Trigui, C. Espanet, A. Bouscayrol, C. Shumei, "Specifications and Design of a PM Electric Variable Transmission for Toyota Prius I", *IEEE trans. on vehicular technology*, vol. 60, no. 9, November 2011, pp. 4106-4114.
- [7] M. S. Rahimi Mousavi, B. Boulet, Modeling, "Simulation and control of a seamless two-speed automated transmission for electric vehicles", *2014 American Control Conference (ACC)* Portland, OR, United States, 4-6 June 2014, pp. 3826-3831.
- [8] X. Zhu, H. Zhang, J. Xi, J. Wang and Z. Fang, "Optimal Speed Synchronization Control for Clutchless AMT Systems in Electric Vehicles with Preview Actions", *2014 American Control Conference (ACC)*, Portland, Oregon, USA, 4-6 June 2014, pp. 4611-4616.
- [9] H. Vahid Alizadeh, M. K. Helwa, B. Boulet, "Constrained Control of the Synchromesh Operating State in an Electric Vehicle's Clutchless Automated Manual Transmission", *IEEE Conference on Control Applications*, Nice, France, 2014, pp. 623-628.
- [10] H. Vahid Alizadeh, Benoit Boulet, "Robust Control of Synchromesh Friction in an Electric Vehicle's Clutchless Automated Manual Transmission", *IEEE Conference on Control Applications*, Nice, France, 2014, pp. 611-616.
- [11] R. Tahmasebi, H. Vahid Alizadeh, M. S. Rahimi Mousavi, B. Boulet, "Robust H_∞ Force Control of a Solenoid Actuator Using Experimental Data and Finite Element Method", *IEEE Conference on Control Applications*, Nice, France, 2014, pp. 1172-1177.
- [12] T. Hofman, S. Ebbesen, L. Guzzella, "Topology Optimization for Hybrid Electric Vehicles With Automated Transmission", *IEEE trans. on vehicular technology*, vol. 61, no. 6, July 2012, pp. 2442-2451.
- [13] G. Lucente, M. Montanari, C. Rossi, "Modelling of an automated manual transmission system", *J of Mechatronics*, Vol. 17, Issues 23, April 2007, pp. 73-91.
- [14] J. Zhang, L. Chen and G. Xi, "System dynamic modelling and adaptive optimal control for automatic clutch engagement of vehicles", *Journal of Automobile Engineering*, vol. 216, December 2002, pp. 983-991.
- [15] A. Ge, H. J. Y. Lei, "Engine Constant Speed Control in Starting and Shifting Process of Automated Mechanical Transmission (AMT)", *FISITA World Automotive Congress*, Seoul, Korea, June 12-15, 2000.
- [16] J. Oh, J. Kim and S. B. Choi, "Design of estimators for the output shaft torque of automated manual transmission systems", *IEEE Conference on Industrial Electronics and Applications (ICIEA)*, Melbourne, VIC, June 2013, pp. 1370-1375.
- [17] J. Oh, S. B. Choi and J. Kim, "Driveline modeling and estimation of individual clutch torque during gear shifts for dual clutch transmission", *J of Mechatronics*, vol 24, 2014, pp. 449-463.
- [18] H. Naunheimer, B. Bertsche, J. Ryborz, W. Novak, "Automotive Transmissions: Fundamentals, Selection, Design and Application", 2nd Edition, Springer, NY, 2011.
- [19] M. Inalpolat and A. Kahraman, "Dynamic modelling of planetary gears of automatic transmissions", *Journal of Multi-body Dynamics*, Part K, vol. 222, Sept 2008, pp. 229-242.
- [20] M. Goetz, M. C. Levesley, and D. A. Crolla, "Dynamics and control of gearshifts on twin-clutch transmissions", *J. Automobile Engineering*, Part D, vol. 219, 2005, pp. 951-963.
- [21] G. H. Jung, B. H. Cho, K. I. Lee, "Dynamic Analysis and Closed-loop Shifting Control of EF-Automatic Transmission with Proportional Control Solenoid Valves", *FISITA World Automotive Congress Seoul*, Korea, 2000, pp. 12-15.
- [22] M. S. Rahimi Mousavi, B. Boulet "Dynamical Modeling and Optimal State Estimation Using Kalman-Bucy Filter for a Seamless Two-Speed Transmission for Electric Vehicles", *23rd Mediterranean Conference on Control and Automation*, Torremolinos, Spain, June 16th-19th 2015, pp. 76-81.
- [23] R. G. Budynas, J. K. Nisbett, "Shigley's mechanical engineering design", 9th Edition, McGraw-Hill, NY, 2011.
- [24] K. Ogata, "Modern Control Engineering", 5th Edition, Prentice Hall, 2009.
- [25] H. K. Khalil, "Nonlinear Systems", third edition, Prentice Hall, 2002.
- [26] G. D. Birkhoff, "Dynamical Systems", American Mathematical Society, Colloquium Publications, 1927.
- [27] S. G. Krantz, "Real Analysis and Foundations", 2nd edition, Chapman and Hall/CRC Press, 2005.